

Pre-calibration of the CMS electromagnetic calorimeter
for the LHC

In partial fulfillment of the
Preliminary Oral Exam

Jason Haupt
Department of Physics and Astronomy
University of Minnesota

Abstract

The Large Hadron Collider (LHC¹) at CERN² is currently under construction in Switzerland. The LHC has been designed to provide high energy interactions so experiments can probe physics at the new energy frontier. The CMS does this through accurate particle identification and energy measurements. The different components of CMS combine together to achieve experimental goals. The electromagnetic calorimeter component is of much importance to the Minnesota group. The precalibration of the crystals will help with the *in situ* calibration with physics events.

1. The Large Hadron Collider

The LHC, will be located near Geneva. At the LHC there will be 5 main experiments, two of which are general purpose detectors, CMS and ATLAS. The beam tunnel has a 27 km radius. The LHC will provide two 7 TeV beams with proton–proton interactions to give a center-of-mass energy of 14 TeV. The expected design luminosity is $10^{34} \text{ cm}^{-2}\text{s}^{-1}$. There will also be lead nucleus–lead nucleus collisions with a total center-of-mass energy on the order of 1 PeV. These specifications were chosen as to enhance the discovery of new physics. Each bunch will be separated in time by 25ns.

The LHC will provide a proton–proton beam. Through careful calculations, using the parton distribution functions (PDF's Figure 1), the rate of a given interaction can be calculated. In order of significance at these energies, the main parton interactions are, gluon-gluon, gluon-valance, gluon-sea quark^α.

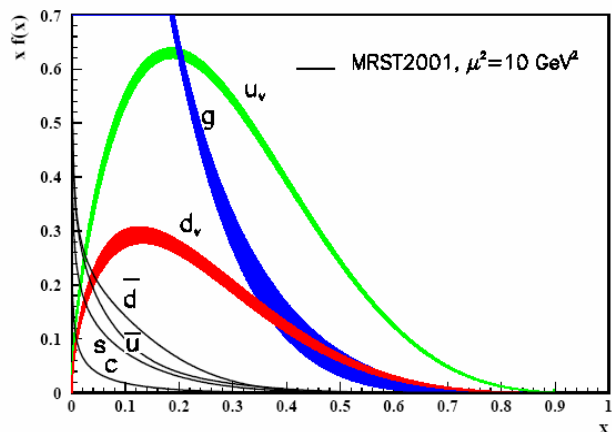


Figure 1¹²

The acceleration process has multiple stages. Protons leave the Cockcroft-Walton (CW) accelerator and get injected into the Linac. Afterwards, the protons get injected into the old proton synchrotron (SP). Next, The super proton synchrotron (SPS) increases the beam energy to 400 GeV. Finally, protons are injected into the LHC ring, and accelerated to the operating energy. Dipole magnets are used to keep the beam in a circular path, and quadropole magnets are used to focus the beam.

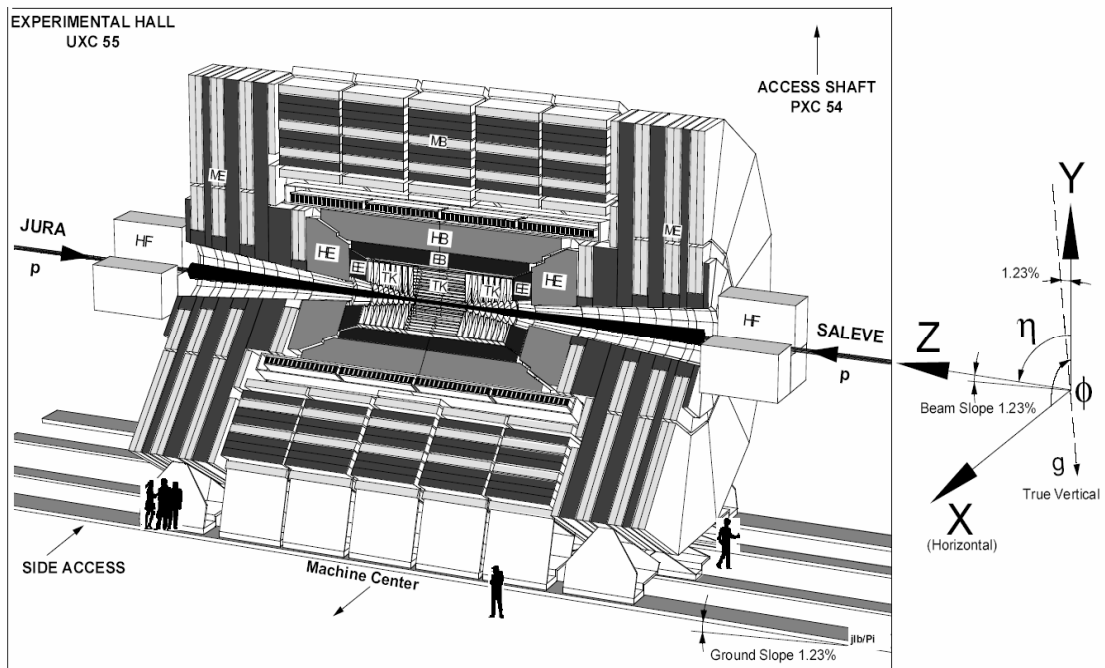
2. The CMS detector

The CMS detector will be at the CERN location of Point 5. This site is near Cessy France. just across the Swiss border from Geneva. Starting from the interaction point, the detector consists of five main components: an inner tracker³, electron calorimeter (ECAL⁴), hadron calorimeter (HCAL⁵), a large solenoidal magnetic field, and a magnetic

^α LHC energies correspond to different PDF's. Energy corresponds to the x value.

return yoke that has interspersed Muon Detectors⁶. The purpose of the different components of a detector such as CMS is multifold. One would be the identification of particles: like photons, electrons, hadrons, muons. Another would be particles found by missing energy (neutrinos and possible SUSY particles). Another would be the measurement of the particle's energy and momentum. Charged particles leave hits in the tracker and experience a force due to the magnetic field. In the ECAL mostly photons and electrons will deposit energy. Photons can be delineated from electrons because photons will not leave a signature in the tracker. Hadrons in general will leave energy in both the ECAL and the HCAL. The shower shape for a hadronic shower is different than electronic shower and can be characterized by such. Muons in general will leave little energy in the calorimeters. Many will leave the detector completely. A good muon system is necessary allowing accurate identification and momentum measurement. 22 events are expected per bunch crossing. Figure 2^β below displays the layout of the CMS detector.

The CMS Detector at point 5 of LHC



Overall view of the CMS detector.

Figure 2⁴

The geometry of the detector is defined generally in 3D with ϕ & η and z . z refers to the direction of the beam pipe. There is some generic $z = 0$ point in the middle of the detector. ϕ refers to the symmetric mostly vertical plane. η is called pseudorapidity and is zero at $z = 0$ and gets progressively larger at larger z . With θ being the standard spherical coordinate with respect to the beam axis. $\eta = -\ln[\tan(\frac{\theta}{2})]$.

^β H = HCAL; E = ECAL; M = Muon; E = Endcap; B = Barrel; F = Forward; TK = Tracker

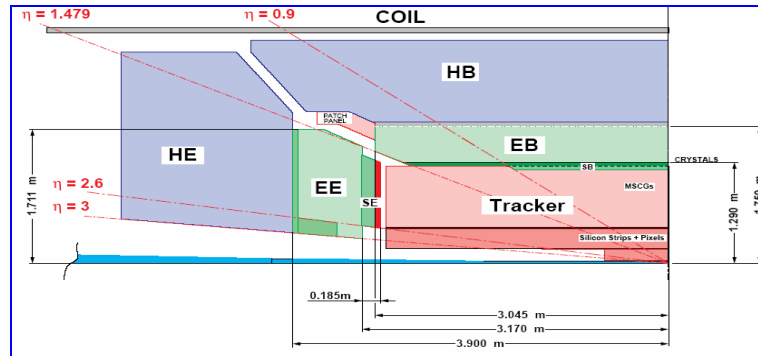


Figure 3⁴. This diagram shows the dimensions and the pseudorapidity coverage of the components that are within the magnet.

2.1 Tracker

The tracker contains two main components, a fine resolution pixel detector at the center and a silicon strip tracker around it. These are both silicon detectors which allow for precise measurements of a charged particle's trajectory. The curvature of the reconstructed track gives a measurement of the particles momentum.

The first detector a charged particle will "see" is the pixel detector. This has the highest resolution with an array of silicon pads, called pixels, allowing for both identification of a primary vertex, and of a secondary vertex. There are 66 million pixels. The pixels yield a spatial resolution of 10 to 20 microns. Surrounding the pixel detector is the silicon microstrip detector. This consists of 15,000 modules. They are readout through sensors and optical fibers. To reduce noise in the harsh radiation environment, the tracker must operate at -10°C .

AREA THICKNESS LAYERS

2.2 ECAL

The purpose of the crystal calorimeter is to have high resolution and be able to accurately reconstruct the energy of the electromagnetic showers. Tolerance in a harsh radiation environment is a must. Excellent granularity, and a fast scintillation time to reduce pileup, are required to produce these goals. e 's & γ 's interact through bremsstrahlung and electron-positron pair production. Lead tungstate scintillating crystals, with a small Molière radius, offer a high homogeneous resolution and allow for a compact calorimeter.

Table 1. Comparing light properties of crystals

	NaI(Tl)	BGO	CSI	BaF ₂	CeF ₃	PbWO ₄
Density [g/cm ³]	3.67	7.13	4.51	4.88	6.16	8.28
Radiation length [cm]	2.59	1.12	1.85	2.06	1.68	0.89
Interaction length [cm]	41.4	21.8	37.0	29.9	26.2	22.4
Molière radius [cm]	4.80	2.33	3.50	3.39	2.63	2.19
Light decay time [ns]	230	60 300	16	0.9 630	8 25	5 (39%) 15 (60%) 100 (1%)
Refractive index	1.85	2.15	1.80	1.49	1.62	2.30
Maximum of emission [nm]	410	480	315	210 310	300 340	440
Temperature coefficient [%/°C]	~0	-1.6	-0.6	-2/0	0.14	-2
Relative light output	100	18	20	20/4	8	1.3

Table 1⁴ shows the advantages of choosing PbWO₄ crystals over other commonly used electromagnetic scintillating crystals.

Lead tungstate crystals (PbWO_4) were chosen for the ECAL detector because they are radiation hard, have a Molière radius of 2.19 cm, and consequently have a small radiation length (X_0 see table 1). The crystals in CMS are about $2.2 \times 2.2 \text{ cm}^2$, and are 23 cm in length ($25.8 X_0$). These contain the electromagnetic shower very well. PbWO_4 also has a light decay time that averages $\sim 10 \text{ ns}$, which is short when bunches are separated in time by 25 ns. This helps prevent pileup. The granularity is $\Delta\eta \times \Delta\phi = .0175 \times .0175$. A high resolution helps detection of the photons in the $H \rightarrow \gamma\gamma$ decay mode. The crystals were also chosen because of their radiation hardness. Barrel crystals will experience around 4 kGy and the endcap crystals 4 – 200 kGy. The dose is a function of η and less for smaller values of η . These numbers are quoted for an expected dose after about 10 years of LHC operation.

There will be over 80,000 crystals in the ECAL (61,200 in the barrel and 21,528 total in the endcaps). The properties in the table 1 show how PbWO_4 compares to other crystals used in electromagnetic calorimeters. PbWO_4 offers all the properties that have been required, but with a low relative light output. Most of the crystals are in the barrel region of the ECAL. This will be constructed of 36 supermodules each with 1700 crystals.

The design of the crystal readout electronics is crucial since a device that has high quantum efficiency, a large collecting area, and possibly gain, would be ideal. The high magnetic field, and high expected radiation dosage, eliminates the choice of some readout devices. The 4 Tesla magnetic field eliminates the use of vacuum photodetectors. The crystals are readout with silicon avalanche photodiodes (APD's). Scintillation of the crystals have too low of a relative light output to use conventional photodiodes. These APD's are operated with a gain of 50 and have a quantum efficiency of 85%. APD's cover $.5 \text{ cm}^2$ of the crystal surface. These APD's are very much like diodes but with a p-n junction that is in reverse-biased mode to provide gain (see figure 4). Electrons get excited by the photoelectric effect (photoelectron = pe) in the p^{++} layer. When the pe reaches the junction, it accelerates under the force due to the large electric field. During

the acceleration of the pe, other electrons are ionized. Therefore, acceleration in this field leads to the avalanche multiplication. APD's are located behind the crystals and in general see a large neutron fluence from the crystals. These neutrons induce some leakage current. This corresponds to an absorbed dose of 13 kGy with a 10 year LHC runtime.

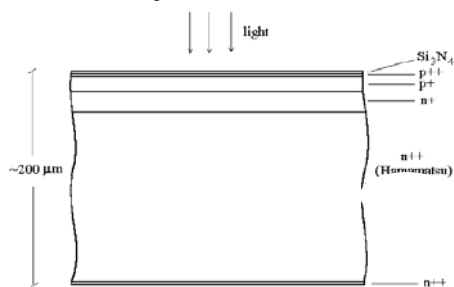


Figure 4⁵

In the ECAL endcaps the same lead tungstate crystals are used, but APD's are not because of the higher amounts of radiation. Instead vacuum phototriodes (VPT's) are used. Here the magnetic field strength is low enough to use vacuum technology. The readout electronics outputs the signal into optical fibers, which are sent into a counting room in the cavern near the interaction point. The granularity of the endcaps becomes progressively worse with higher η . The η coverage can be seen in figure 3.

2.3 HCAL

Hadrons, mostly pions, reach the HCAL. Other hadrons include protons, neutrons, and kaons. A properly designed calorimeter allows for the measurement of energy and position. As was mentioned earlier, hadronic showers have a different shape than electromagnetic showers, they tend to develop later and have larger dimensions. For these reasons, HCAL is much larger than ECAL.

The barrel HCAL is composed of alternating plates of brass and plastic scintillators with wavelength shifter readout done by photosensors. These are essentially hybrid photodiodes. The forward hadronic calorimeter (HF see figure 2) is located on both sides of the barrel region and is basically wedges of steel plates with many quartz fibers. Some of these fibers are slightly shorter than the others. These radiation hard quartz fibers are read out with standard type PMT's. These are used because they are radiation hard and the HF is far enough out of the peak of the magnetic field where the use of PMT's is acceptable.

2.4 Solenoidal Magnet

The magnet is not a standard idea of a detector component. However, a magnet plays a critical role in the CMS design. The 4 Tesla solenoid surrounds the tracker, ECAL and HCAL. The magnetic field is essential for determining charged particles from electrically neutral particles. The magnetic field also allows for measurement of momentum. 4 Tesla is achieved with special cables with an operating current of 19.5 kA. To dump all the energy, there are a few options, such as a very large (300MW) resistor. The outer yoke of the magnetic coils contains the muon chambers and have a ~ -1.8 T field^z.

2.5 Muon Detectors

The muon chambers make up the largest part of the CMS detector. They are critical because detection of muons leads to proper reconstruction of an event. Full reconstruction allows for the accurate measurement of missing energy. Also muons appear on a popular decay chain the standard model Higgs boson. Three different muon detectors are used. These are drift tube (DT) chambers in the barrel region, cathode strip chambers (CSC) in the endcaps, and some resistive plate chambers (RPC) that are on the DT and CSC chambers. There are four layers of these DT or CSC. DT chambers are tubes of wires that work in 8-12 layers. CSC's are multiwire proportional chambers with cathode strips and anode wires, which run parallel to the strips. The main purpose of the RPC's is to have accurate time measurements that are less than the spacing between bunch crossings.

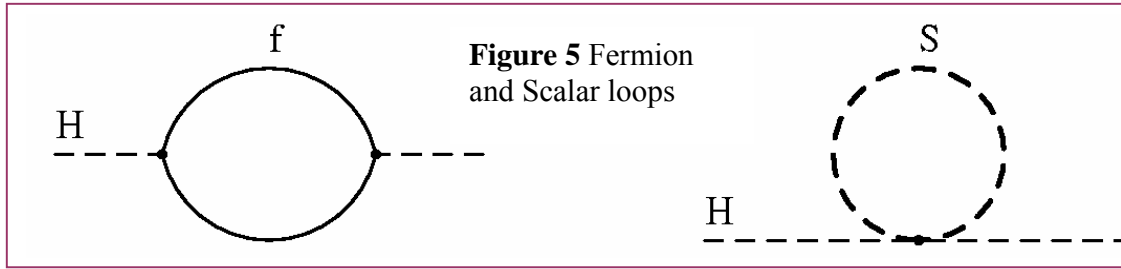
3. CMS Physics Frontier

There will be many new opportunities to explore the physics at the LHC energy scale. One of the major elements of the standard model (SM^δ) is the Higgs particle. This particle is a boson that gives mass to all other particles. Its much-anticipated detection would be a great confirmation to the SM. The hierarchy problem is that the correction to the mass squared of the Higgs boson is proportional to the square of the ultraviolet cutoff

^z This is negative with respect to the direction inside the solenoid.

^δ In this section only SM refers to standard model.

to first order and logarithmically to the UV cutoff to the next order (see equations 1 & 2). These equations are calculated from the simple Higgs coupling terms in the Lagrangian. These are just the one loop diagrams assuming that there is a momentum cutoff (Λ_{UV}^2). This is a large problem in the SM because the Higgs particle must be light enough to give the masses that we see for the other SM particles. This would not be the case if the ultra violet cutoff were to be near the Planck mass ($M_p \sim 2 \times 10^{18}$ GeV). Below is the correction to the Higgs mass for a fermion and complex scalar loops⁽¹²⁾. Equation 3 shows the combination of the a Dirac fermion term and two complex scalar terms.



$$\Delta m_H^2 = \frac{|\lambda_f|^2}{16\pi^2} \left[-2\Lambda_{UV}^2 + 6m_f^2 \ln[\Lambda_{UV}/m_f] + \dots \right] \text{ eq. 1}$$

$$\Delta m_H^2 = \frac{\lambda_s}{16\pi^2} \left[\Lambda_{UV}^2 - 2m_s^2 \ln[\Lambda_{UV}/m_s] + \dots \right] \text{ eq. 2}$$

$$\Delta m_H^2 = \frac{\Lambda_{UV}^2}{8\pi^2} \left[\lambda_s - |\lambda_f|^2 \right] + \dots \text{ eq. 3}$$

There are a few proposed solutions to this problem. One solution would be to say that there are as many fermions as bosons of the same type since the UV quadratic term is also proportional to the coupling constants of the particles^ε. This would eliminate the quadratic term in the Higgs mass and thus solve the hierarchy problem. One way of doing this is introducing a boson for every fermion and visa versa. This solution is actually a natural result of supersymmetric theories (SUSY), which start with the general assumption of the extended Coleman-Mandula theorem. There is a generator that turns a fermion into a boson and visa versa. This operator and the others of the gauge group must satisfy a graded Lie algebra with commuting and anti-commuting operators. Other solutions to the hierarchy problem are fine tuning all the different terms so they just happen to cancel in a very unnatural way, or large extra dimensions that lower the value the UV cutoff.

Since the supersymmetric counterparts of the SM particles have not been observed^φ, SUSY must be a broken symmetry. The three most common SUSY breaking mechanisms are, gauge mediated, anomaly mediated, and gravity mediated. The most commonly

^ε More precisely, the number of fermionic degrees of freedom must equal the number of bosonic degrees of freedom.

^φ This statement refers to SUSY particles not being observed to have the same mass as the standard model particles. Most (all but the larger mass counterparts) can be eliminated by known observations. As an example, a charged scalar with the mass of the electron has not been observed.

referred to is the gravity mediated SUSY breaking. This method is preferred for reasons that gravity is believed to unify with the SM forces at large energies. If the scale of the SUSY particles were much larger than 1 TeV, corrections to the standard model particles would be too large⁷.

The two most likely decay modes of the Higgs boson that can be investigated would be $H \rightarrow \gamma\gamma$ & $H \rightarrow 4$ leptons. This first decay mode is the reason for such fine granularity of the ECAL, because the detection of photons for this decay is critical. The two photon decay is favored for low mass Higgs ($m_H < 150$ GeV). The 4 lepton and other decays are favored for a higher mass Higgs ($140 \text{ GeV} < m_H < 700 \text{ GeV}$) which can decay into Z and W vector bosons².

Another interesting result of SUSY is that if R-parity (baryon – lepton number conservation) is relatively good, then there must be a SUSY particle, which cannot decay. R-parity is currently well confirmed by the limits set on the decay of protons. If this particle is neutral, then the particle can be a massive dark matter constituent. The particle would be called the lightest supersymmetric particle (LSP). The LSP cannot be detected directly, since it doesn't decay. The LSP would most likely be found through a decay of the next lightest supersymmetric particle (NLSP).

3. ECAL Detector Component Calibration

Long before physics results at the new frontier can be stated, the value of the measurement needs to be fully understood. For very high energy processes, the ECAL will be calibrated with the well understood decay of the neutral vector boson $Z \rightarrow e^+ e^-$. This is well understood because of the precise LEP¹¹ measurement of the width and error for this decay. In fact, so precise that CMS will be unable to reach that resolution. With such a precise measurement an ECAL zone of 400 crystals can be calibrated to within 0.3%. Calibration can also be done at low energies with processes like $\pi^0 \rightarrow \gamma\gamma$. This calibration may be possible with an order of 1 day's worth of statistics. The *in situ* calibrations require the intercalibration constants to be known within 2%. This would allow for a much quicker inversion of an 80,000 by 80,000 calibration matrix. There are a few ways of extracting the intercalibration constants.

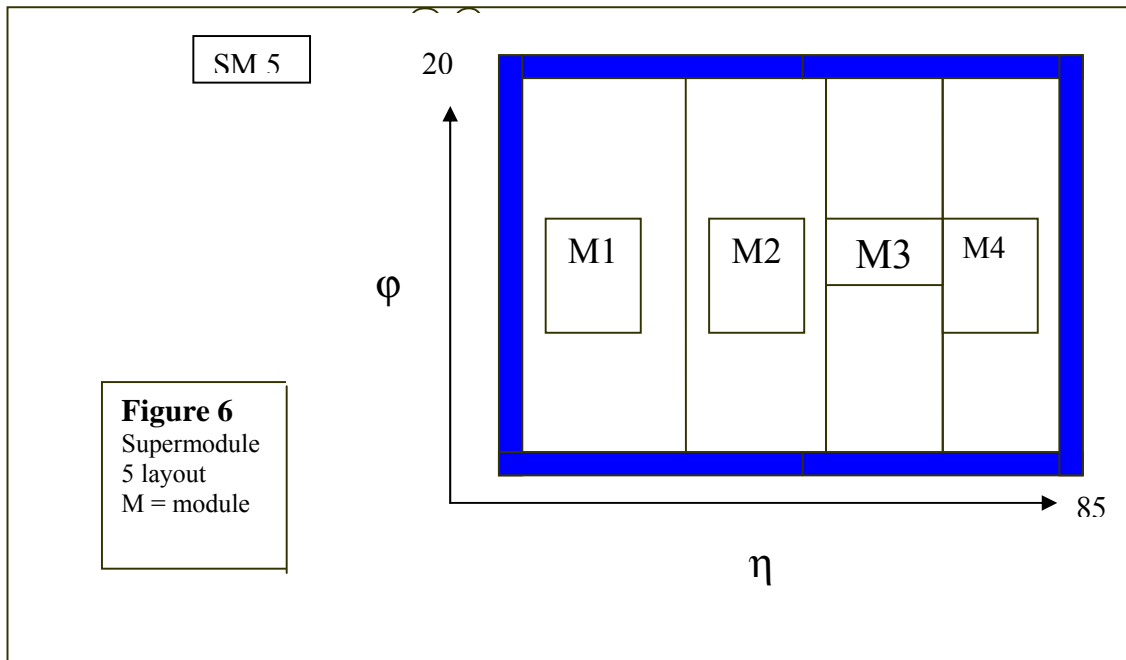
1. Direct laboratory measurements of each detector component.
2. Test beam Measurements with particles of known energy.
3. Muons from cosmic rays.

The first one will be done for each supermodule. This allows for an order of 4% error in the inter-calibration coefficients. The most optimal thing to do would be to perform the second method as well. This is a large problem because providing test beam for each supermodule is no longer practical with the current experimental timetable. The third option then becomes not only a check of the laboratory measurements, but also a way to reduce the total precalibration error.

⁷ The logarithmic term in the SM vector's mass correction would require fine-tuning if the SUSY scale were too large. See eq. 1

4.1 Cosmic Setup

A supermodule (SM)¹ contains 1,700 crystals arranged in a 20 by 85 structure with labels called ϕ and η respectively². The SM is further divided into 4 modules each of either 400 or 500 crystals. Each module is further divided into sub modules of 2x5 crystals. The module in the lowest η range is called module 1, and the highest η values are referred to as module 4. The layout is below in figure 6.



An incoming muon triggers the data collection process (DAQ). A scintillating pad, a short distance from the SM, defines an interaction point. At least one of the 6 counters that are distributed over the bottom is required to have fired within a reasonable amount of time. This coincidence triggers the readout of all crystals in the SM. There are also 6 scintillators on the top of the supermodule. The top counters eliminate the need for a tracker during pre-calibration. See figure 7 for the trigger diagram.

Importance is placed on the DAQ process and on the data format. The current DAQ system is very close to what the final system will be. The values are read out in ADC counts with a pedestal value around 200 ADC counts. 1 ADC count corresponds to ~ 9 MeV. The crystal, timing, and scintillator data are output into Root⁷ files that are easily read within ECAL's H4Ana⁸ framework. This was specifically implemented for ECAL calibration. The general Root framework is also used.

¹ From this section on SM refers to supermodule.

² For the purposes of the cosmic setup, η and ϕ , correspond to coordinates in the direction of η and ϕ . Integer units are used to simplify the software and analysis to intercalibrate each SM separately.

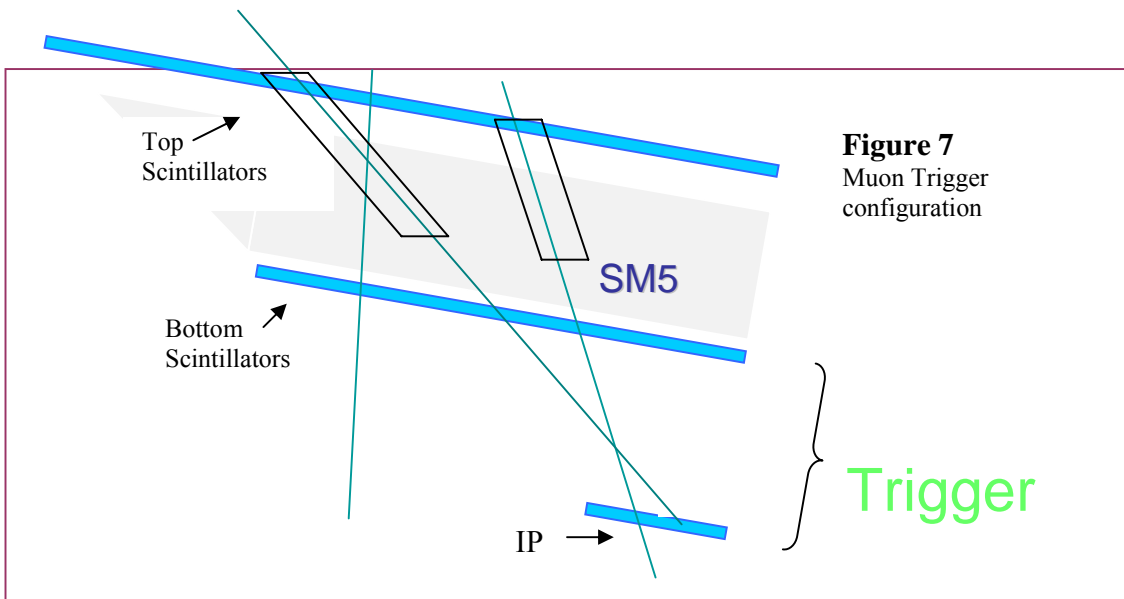
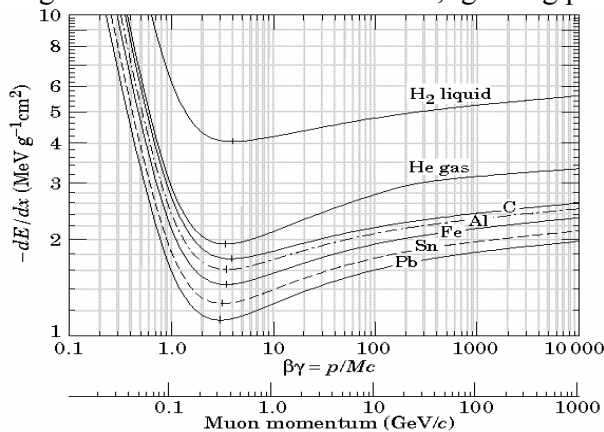


Figure 7
Muon Trigger configuration

Because of the high resolution, it is not necessary to track the muons (μ 's) before or after the SM. Muons are minimum ionizing particles (MIPs). Meaning that for the energy range of most of the cosmic muons, ignoring part of the relativistic rise in the dE/dx



curve, μ 's leave the same amount of energy per unit distance. Figure S displays the features of a MIP. A MIP in the ECAL has a $-dE/dx \sim 11$ MeV/cm. A μ going through a 23 cm long crystal deposits about 250 MeV. This physics process then provides a good way of inter-calibrating the crystals. This process requires that a good noise rejection is achieved as well as a muon must traverse only one crystal.

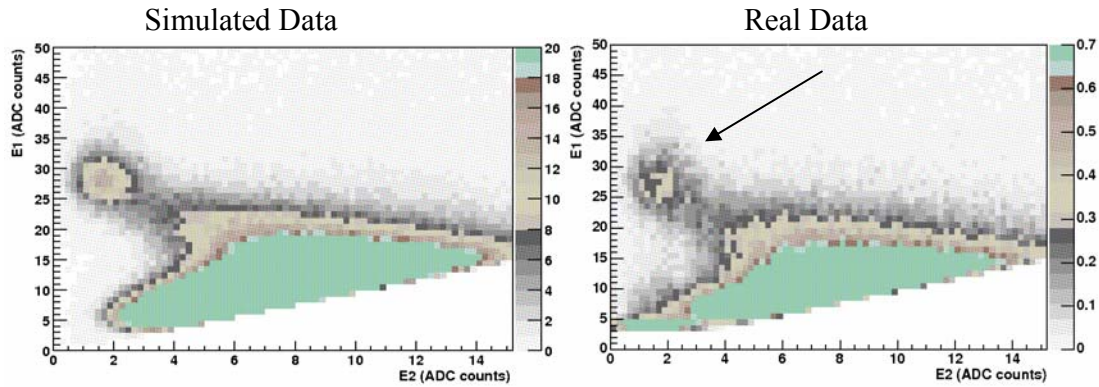
Figure 8⁽⁹⁾

Above is a plot of what $\frac{dE}{dx}$ looks like for a muon based on the Bethe-Bloch equation.

4.2 Cosmic Selection

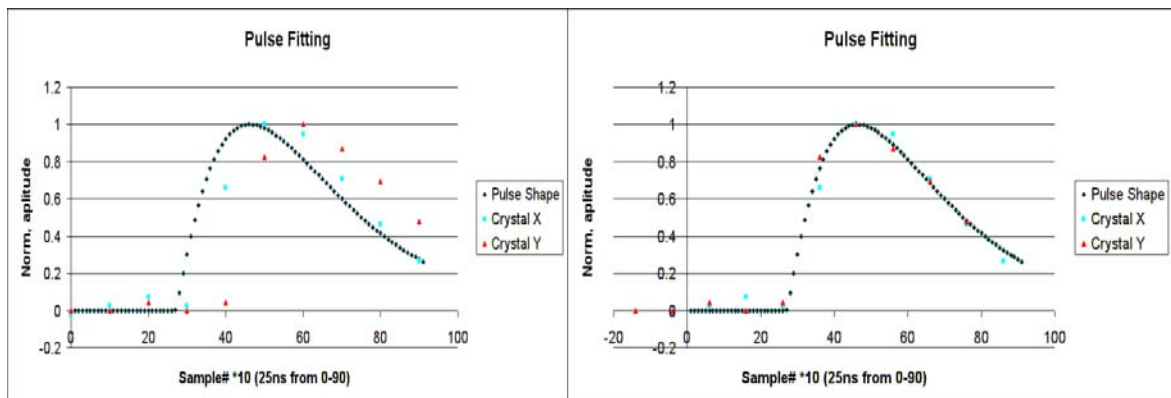
One of the first major steps in the cosmic calibration is the selection of events. The first selection would be to select candidates that only went through a single crystal. This can be achieved for most of a SM by looking at the surrounding crystals. With E1 being the energy of the highest crystal, and E2 being the energy of the (3, 5, or 8) adjacent crystals, one can see in the histogram below (Figure 9) specific cuts allow selection of events that correspond to a muon going through one crystal. These cuts are the E1 must be larger than 10 ADC counts, and that each of the E2's must be less than 3 ADC counts.

Figure 9⁽¹⁰⁾ Simulated data vs. real data on selecting and aligned μ .



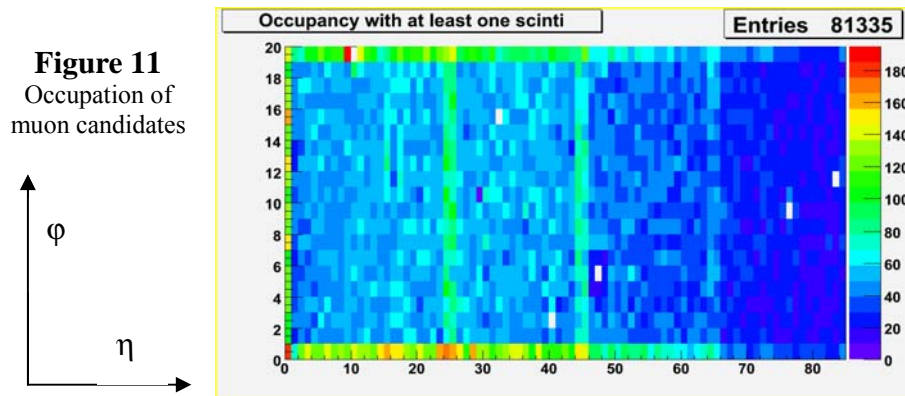
Only the most energetic particle is chosen in a triggered event. For each crystal there are 10 samples over a 25 ns period. The crystal with the maximum ADC sample in time is selected. A comparison of event samples to pulseshape can be done. This comparison allows for the elimination of most noisy channels. The compared pulseshape is either from lab or from testbeam. The shape can be sampled with the laser and pulse system. The selection for the rest of the paper included the use of a least squares fitting approach. Events with a Chi-sq greater than 5 were eliminated (see figure 10). Events, whose maximum sample did not correspond to the 5th or the 6th time sample, were also eliminated. Based on the triggering system mentioned before, physics particles only appear in those samples. An example of a hot electronic ADC count could appear in the second sample, but not in any of the other samples. The process mentioned thus eliminates this hot count.

Figure 10 Left is before the pulse fitting, right is after the pulse fitting.



These two selection criteria define the muon candidates. This selection yields higher amounts of candidates in both the edges of the SM and the regions between the different modules (see figure 11). The larger number of events in for these crystals is a direct result of using the 3 or 5 surrounding crystals to find aligned μ 's. The excess of events in the module borders is acceptable because the noise is small enough to allow a fit. Edge crystals have the peak of the candidates surrounded by a lot of noise (looking at a

histogram of E1 in time). Scintillating pads around the edge of the SM border are used to reduce the background. Using these coincidences with the top counters, muons can be found that primarily went through just an edge crystal, and not partially through an edge crystal.



4.3 Cosmic Calibration

In order to achieve good statistics for a given crystal ~ 100 aligned muon candidates are needed. A nominal time of 1 week of integration is expected for each SM. About $130 \text{ muons} \cdot \text{m}^{-2} \cdot \text{s}^{-1}$ incident, yield about 61 ± 2 events/crystal/day after the cosmic selection. Though only about 55 ± 2 are seen, this is most probably caused by a combination of not understanding the incident muon flux and the efficiencies of the scintillating pads. Good statistics implies intercalibration constants to be known with a better than 3% error.

The SM itself has some internal crystal geometry; not all crystals are aligned in the same direction. There is a progressive tilt as a function of η . This tilt is greater between each of the modules. Module 4 has the largest tilt with respect to module 1. To overcome this tilt, the SM itself has a slight tilt to it to increase the statistics of the 4th module at the cost of the some of the statistics in the 1st. The SM has been tilted 10 degrees for this very reason.

Each ring of η is expected to have the same distribution, neglecting edge crystals. The average of 18^λ crystals in a given η ring produces a distribution. Each crystal can be fit to the distribution histograms with normalization and energy scale factor as the only tunable parameters. This currently results in 2.5% relative difference of intercalibration constants in module 1, to about 3.5% in module 4. These can be combined with laboratory measurements in order to find collective calibration constants.

4.4 Current Cosmic Work

The efficiency of the top counter aligned muon tagging procedure deserves some attention. Figure 12 shows the fraction of aligned muon candidates that had a hit in a top counter for each crystal. One observation would be that the top scintillators may not be positioned optimally to achieve proper tagging statistics. The other is that the efficiency

^{λ} The two edge crystals are ignored.

of the scintillators may cause an asymmetry in the ϕ edges. This has resulted in fewer statistics in the $\phi = 20$ edge than in module 4. The current resolution to these problems has been to reposition the top counters and to turn up the high voltage on the top counters. The HV increase has had the most dramatic impact and has led the $\phi = 20$ edge to have similar statistics to that of module 4.

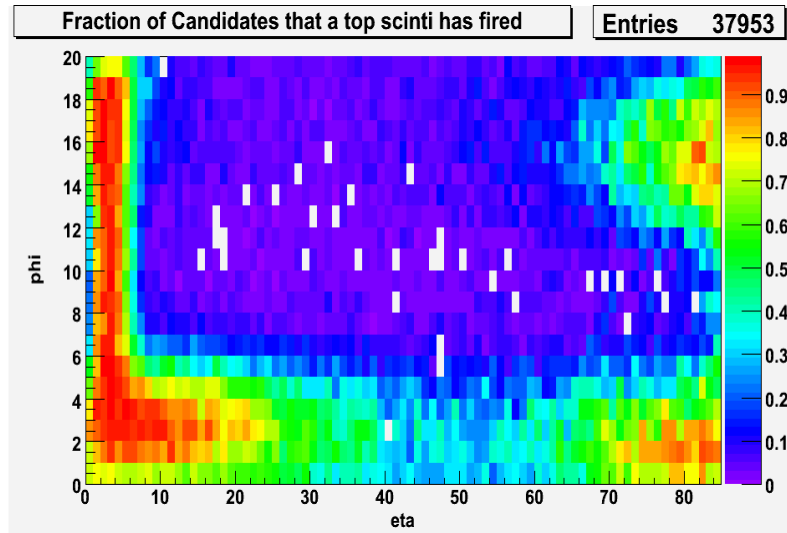


Figure 12

5. Acknowledgements

A special thanks to Professor Roger Rusack for his comments on writing this document.

6. References

1. CMS Collaboration <http://cmsinfo.cern.ch>
2. CERN: <http://cern.ch/public>
3. CMS Collaboration, The Tracker Project, TDR CERN/LHCC 98-6
<http://cmsdoc.cern.ch/cms/TDR/TRACKER/tracker.html>
4. CMS Collaboration, The Electromagnetic Calorimeter Project, TDR CERN/LHCC 97-33 <http://cmsdoc.cern.ch/cms/TDR/ECAL/ecal.html>
5. CMS Collaboration, The Hadronic Calorimeter Project, TDR CERN/LHCC 97-31
<http://cmsdoc.cern.ch/cms/TDR/HCAL/hcal.html>
6. CMS Collaboration, The Muon Project, TDR CERN/LHCC 97-32
<http://cmsdoc.cern.ch/cms/TDR/MUON/muon.html>
7. Root Project <http://root.cern.ch>
8. H4Ana Framework <http://cmsfrance.in2p3.fr/h4ana/>
9. S. Eidelman *et al.*, Phys. Lett. B **592**, 1 (2004)
<http://pdg.lbl.gov/2005/reviews/passagerpp.pdf>
10. A not yet published CMS note: M. Bonesini *et al.* Pre-Calibration of the CMS electronic calorimeter with cosmic rays.
11. LEP Collaboration. See CERN.
12. S. P. Martin. A Supersymmetry Primer. hep-ph/9709356 v3 April 7, 1999